Journal of Optoelectronics and Advanced Materials Vol. 7, No. 4, August 2005, p. 1813 - 1821

A STUDY OF THIN AMORPHOUS (Ag)-Sb-S FILMS PREPARED BY THERMAL EVAPORATION COMBINED WITH OPTICALLY INDUCED DIFFUSION AND DISSOLUTION OF SILVER

J. Gutwirth, T. Wágner*, S. O. Kasap[a], M. Frumar

University of Pardubice, Department of General and Inorganic Chemistry and Research Centre LC532, Legion's sq. 565, 53210 Pardubice, Czech Republic
[a]University of Saskatchewan, Department of Electrical Engineering, Campus Dr. 57, Saskatoon S7N 5A9, Canada

There were prepared thin amorphous films of ternary system Ag-Sb-S as potential candidate for a new phase-change memory recording layer. In the first step, there were prepared two host Sb-S films on glass substrate by thermal evaporation using two different rates. Silver films were "step-by-step" consecutively evaporated on top of the Sb-S host films. Each evaporation step was followed by illumination. This process (Optically Induced Diffusion and Dissolution of Ag) produces two set of samples with different Ag dissolution limit. All (Ag)-Sb-S thin films are homogeneous amorphous and with good optical quality. Prepared films were characterized by SEM-EDX analysis, MDSC analysis, UV-VIS-NIR and Raman spectroscopy. Amorphous character was checked by SEM and by XRD. Influence of preparation conditions or silver content on physico-chemical properties (composition, optical and thermal properties, maximum silver content) is discussed.

(Received May 19, 2005; accepted July 21, 2005)

Keywords: Chalcogenide glasses, (Ag)-Sb-S, MDSC

1. Introduction

Current research of suitable materials for rewritable (RW) optical data recording (ODR) is now focused on the group of chalcogenide materials. Typically studied materials in this time are doped Sb-Te [1] alloys. For example materials such a Ge-Sb-Te (GST) [2] or Ag-In-Sb-Te (AIST) [3] are widely used as active recording layer in commercially used rewritable (RW) data storage media e.g. CD-RW and DVD-RW.

Requirements for optical properties of RW-ODR materials are [4] sufficient optical contrast between amorphous and crystalline phases for wavelength used in data reading process and sufficient absorption for writing/erasing wavelength. Requirements for thermal properties of RW-ODR materials are low melting point (500°C – 1000°C, typically ~ 600°C), stability against self crystallization during storage as well as during writing. It is means, that the glass transition temperature must be over 100 °C. Good stability of amorphous and crystalline phases is also required for achieving good cyclability (changes between crystalline and amorphous state and vice versa) of material as well as high crystallization rate.

Increase of storage capacity [4,5] is also intensively studied in these days. Several methods and techniques exist to reach higher capacity. First approval is based on modification of media, i.e. layer structure modifications of disks [1] or usage of double sided and/or double layered media [6]. Second possibility is based on increasing of recording density; it is techniques as Land-Groove

* Corresponding author: Tomas.Wagner@upce.cz

recording [4] which increases radial density, short wavelength recording [7], recording with high numerical apertures (NA) optics [8] or fiber optical head [9] and recording by femto-second lasers [10]. Third option is based on change of write/read technique. Techniques as Mark-Edge recording [11] and Mark Radial Width Modulation recording (MRWM) [12] can be inserted to this category.

Current usage of short wavelength lasers for ODR (e.g. Matsushita Blu-Ray disc technology) allows utilize materials such as Selenium or Sulfur based chalcogenides as recording layer.

Our previous work was focused on study of OIDD kinetic [13] and Ar^+ ion laser induced photocrystallization of (Ag)-Sb-S thin films. Influence of preparation method and silver content on photocrystallization process [14] was also studied.

The aim of this work is to study thermal (glass transition temperature T_g, crystallization temperature T_c, melting temperature T_m) and optical (band gap energy E_g^{opt}, refractive index n) properties of Ag-Sb-S thin films prepared by thermal evaporation of Sb-S combined with optically induced diffusion and dissolution (OIDD) of Ag. Influence of composition and structure is also studied.

2. Experimental

There were prepared bulk of Sb-S. This bulk was synthesized in precleaned ampoule from pure elements of Sb and S. Ampoules were evacuated to residual pressure ~ 5×10^{-3} Pa. Synthesis temperature was 750 °C for 24 hours and crystalline bulk was obtained by quenching in water. Stoichiometry of prepared bulk was $Sb_{33}S_{67}$.

Thin films were prepared by thermal evaporation with planetary rotation of substrates (microscope slides) to provide constant thickness and homogeneity of prepared thin films. Deposition rate and thickness of films were monitored by quartz crystal monitor. Thermal evaporation were carried out under vacuum ~ 10^{-4} Pa, deposition rate were 2 nm×s^{-1} (b2 samples) and 10 nm×s^{-1} (b10 samples). Thicknesses of Sb-S films were 700 - 800 nm.

Prepared thin amorphous Sb-S films were consecutively photodoped by silver. Constant thickness silver layers (5 nm Ag for b2 samples and 10 nm Ag for b10 samples) were thermally evaporated on surface of Sb-S host matrix and consecutively illuminated by 500 W tungsten lamp focused by large Fresnell lens with IR-cut filter. This process (Step by Step Optically Induced Diffusion and Dissolution of Ag) provides sets of samples with different Ag content. Thin amorphous Ag-Sb-S films prepared by this technique are homogeneous and good optical quality (proved by UV-Vis-NIR spectroscopy, SEM-EDX and XRD).

Composition of prepared films were traced by SEM-EDX analysis on SEM apparatus Jeol JSM - 5500 LV with analyser IXRF Systems and detector Gresham Sirius. Accelerating voltage was 20 kV, minimal measurement time depend on Ag content and was longer than 60 s.

Structure of prepared films was studied by Raman spectroscopy. Raman spectra were carried out on FT Raman spectrometer Bruker IFS/FRA 106 with Nd-YAG excitation laser (λ = 1064 nm). There were realized 100 scans with output laser power 50 mW and resolution 4 cm^{-1}. Thin films were mechanically peeled from the substrates and then put into Al targets for Raman measurements.

Optical transmission spectra were recorded on UV-Vis-NIR spectrophotometer Jasco V-570. Resolution of spectrophotometer was 2 nm. Spectral data were evaluated by Swanepoel method [15] (to acquire film thickness d, refractive index n and absorption coefficient α) and by Tauc extrapolation [16] to get E_g^{opt} value. Software WinSwan ver. 1.01 developed in University of Pardubice were used for this evaluation.

Thermal data were obtained from MDSC measurements. These measurements were carried out on apparatus TA Instruments DSC-Q100 (b2 samples (see Table 1)) and apparatus TA Instruments DSC-2910 (b10 samples (see Table 1)) with declared sensitivity 0.2μW. Temperature gradient was 5 °C×min^{-1}, amplitude of temperature modulation was A = ±1 °C and

modulation period was 60 s in both case. Typically weight of sample was ~ 1 mg (b2 samples) and ~ 5 mg (b10 samples).

Amorphous character of prepared films was checked by μ-XRD and SEM techniques [17].

3. Results

There were prepared two sets of samples in (Ag)-Sb-S system by thermal evaporation of $Sb_{33}S_{67}$ bulk combined with optically induced diffusion and dissolution of silver. Identification of samples and their properties (composition, film thickness d and band gap energy E_g^{opt}) are summarized in Table 1. Sb-S host matrix of the first set of samples (b2) was prepared by thermal evaporation of $Sb_{33}S_{67}$ bulk at a rate 2 nm × s^{-1} and Sb-S host matrix of the second set of samples (b10) by thermal evaporation of $Sb_{33}S_{67}$ bulk at a rate 10 nms^{-1}. Both host matrixes were consecutively photodoped by silver. Photodissolution Ag limit for b2 set of samples is only 3.5 at.%, for b10 set of samples is 11.2 at.% respectively.

Table 1. Identification of samples and thin films composition, thickness and optical band gap energy E_g^{opt}.

Sample	Composition [at %]	d [nm]	E_g^{opt} [eV]
b10-0	$Sb_{33}S_{67}$	805.3	1.847
b10-10	$Ag_{2.3}(Sb_{33}S_{67})_{97.7}$	726.0	1.798
b10-20	$Ag_4(Sb_{33}S_{67})_{96}$	761.0	1.751
b10-30	$Ag_{5.4}(Sb_{33}S_{67})_{94.6}$	747.8	1.725
b10-40	$Ag_{8.2}(Sb_{33}S_{67})_{91.8}$	791.9	1.675
b10-50	$Ag_{10.7}(Sb_{33}S_{67})_{89.3}$	798.5	1.641
b2-0	$Sb_{40}S_{60}$	721.7	1.665
b2-5	$Ag_{1.1}(Sb_{40}S_{60})_{98.9}$	730.0	1.605
b2-10	$Ag_{2.4}(Sb_{40}S_{60})_{97.6}$	744.3	1.582

Raman spectra are presented in Fig. 1. (b2 samples) and Fig. 2. (b10 samples). Raman spectra were interpreted on basis of Watanabe's paper [18]. Strong band at 292 cm^{-1} correspond to vibrations of $SbS_{2/3}$ units, band at 170 cm^{-1} correspond to vibrations of Sb-Sb in S_2Sb-SbS_2 units and bands 140 cm^{-1} and 475 cm^{-1} correspond to vibrations S-rings fragments.

There are UV-Vis-NIR transmission spectra of prepared (Ag)-Sb-S amorphous thin films on Fig.3. (b2 samples) and Fig. 4. (b10 samples). Detail of short wavelength range (absorption edge area) for b10 samples is presented in Fig. 5. Transmission spectra (relative transmittance T vs wavelength λ) were evaluated by Swanepoel method [15] and by Tauc extrapolation [16]. Results (film thickness d, band gap energy E_g^{opt},) are summarized in Table 1. Spectral dependences of refractive index are presented in Fig. 6. (b2 samples) and Fig. 7. (b10 samples).

DSC curves are presented in Figs. 8. and 9. (b2 samples) and Figs. 10. and 11. (b10 samples). Figs. 9. and 11. represents details of T_g region of DSC curves. Results of MDSC measurements are summarized in Table 2.

DSC curves show decrease of T_g value with increasing silver content for both sets of samples b2 and b10, respectively (Figs. 8.-11.).

In case of b2 samples is visible decrease of $T_c(Sb_2S_3)$, $T_c(Ag_3SbS_3)$, $T_m(Sb_2S_3)$ and $T_m(Ag_3SbS_3)$ values (Figs. 8 and 9). DSC peaks interpretation is rather difficult in case of b10 samples (Figs. 10. and 11.). Crystallization temperature $T_c(Ag_3SbS_3)$ simply decreases with

increasing silver content, but $T_c(Sb_2S_3)$ values show some fluctuations. First is step increase of $T_c(Sb_2S_3)$ value after first silver doping (between b10-0 and b10-10 samples), second one is increase of $T_c(Sb_2S_3)$ values which starts in region of cca ~ 8.2 at % of Ag (b10-40 sample). These irreguralities in $T_c(Sb_2S_3)$ values vs Temperature dependence will be discussed below.

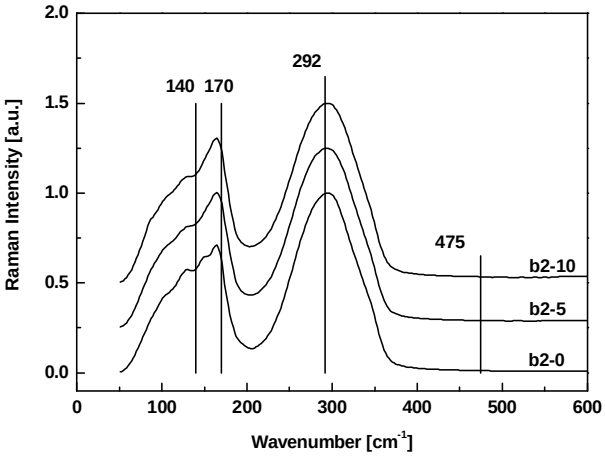

Fig. 1. Raman spectra of b2 samples.

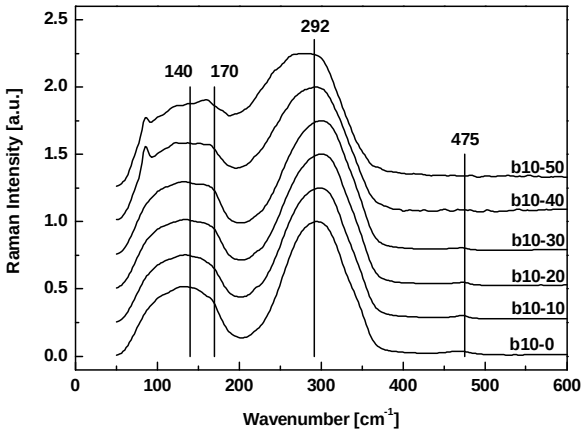

Fig. 2. Raman spectra of b10 samples.

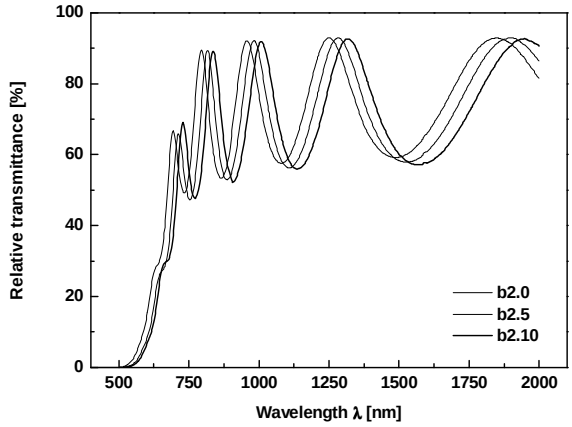

Fig. 3. Optical transmission spectra of prepared b2 (Ag)-Sb-S thin amorphous films.

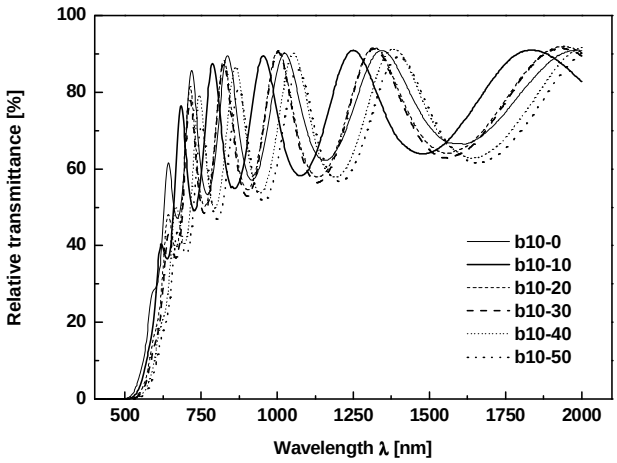

Fig. 4. Optical transmission spectra of prepared b10 (Ag)-Sb-S thin amorphous films.

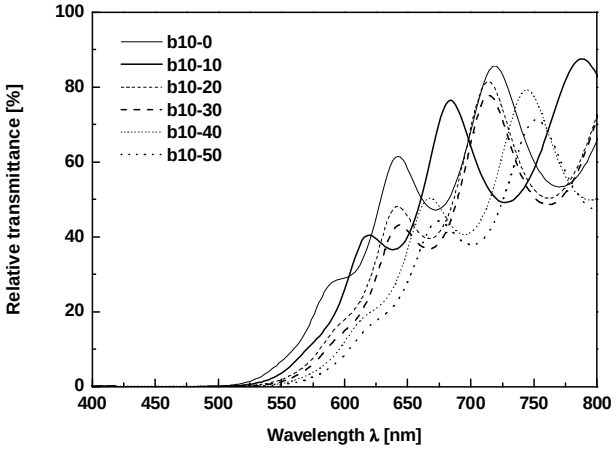

Fig. 5. Detail of absorption edge area of prepared b10 samples.

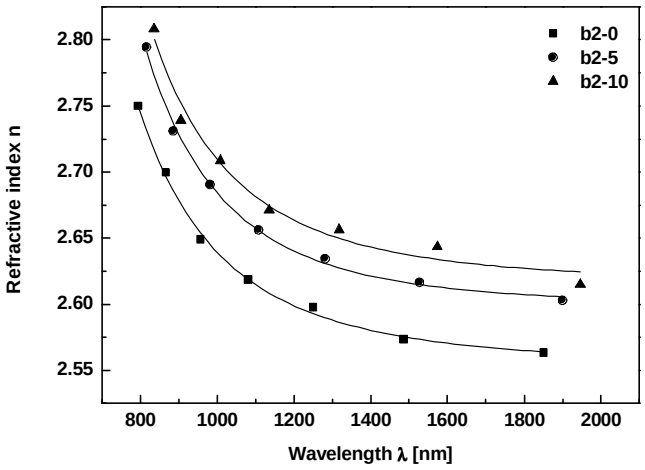

Fig. 6. Spectral dependence of refractive index of b2 samples.

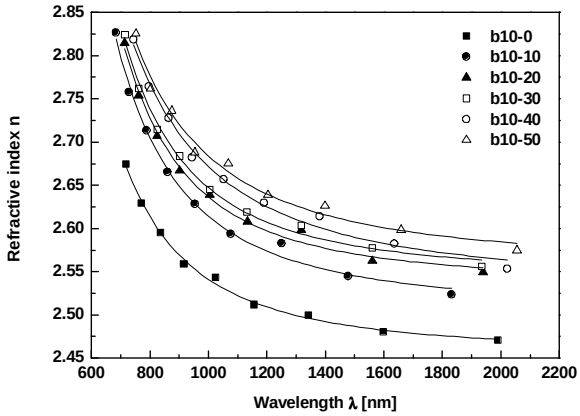

Fig. 7. Spectral dependence of refractive index of b10 samples.

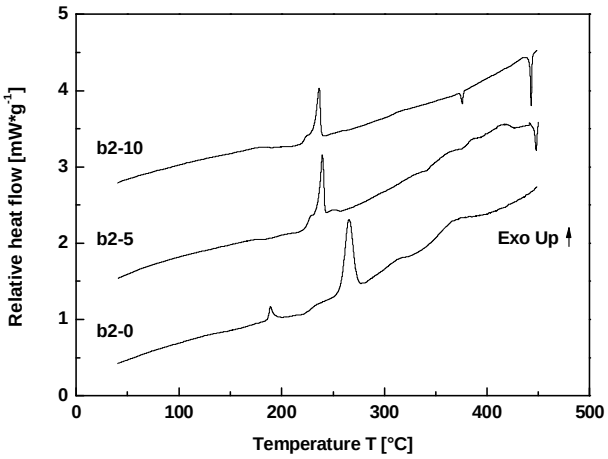

Fig. 8. DSC curves of b2 samples.

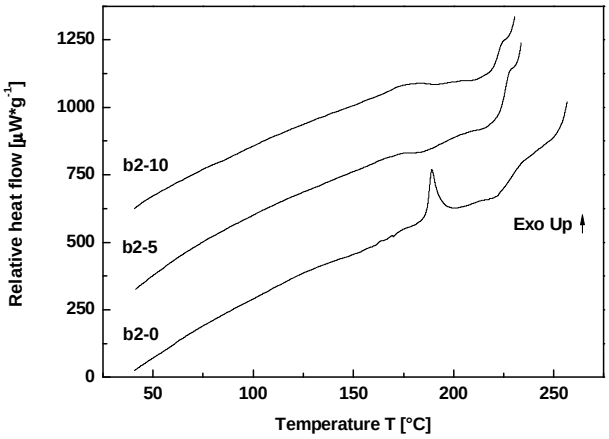

Fig. 9. T_g region of DSC curves of b2 samples.

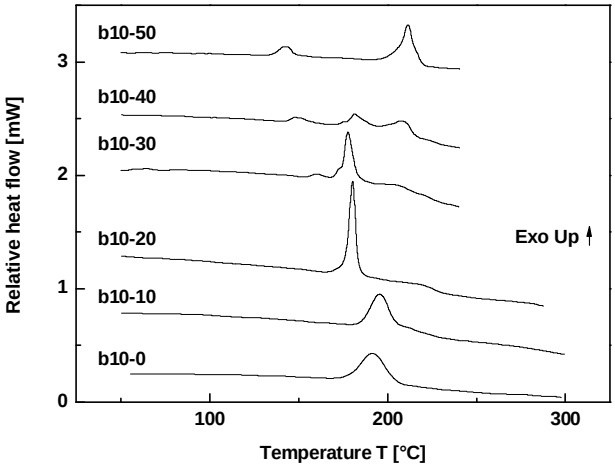

Fig. 10. DSC curves of b10 samples.

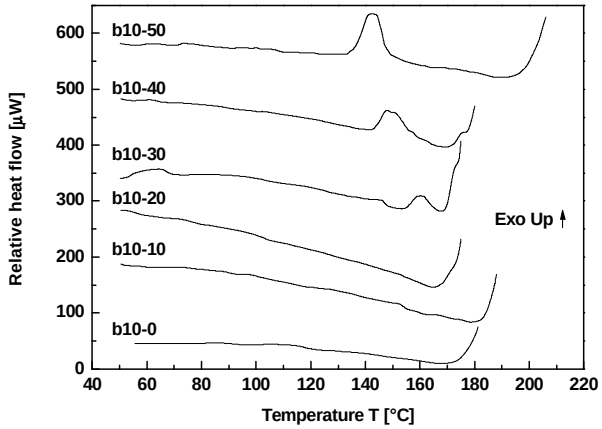

Fig. 11. T_g region of DSC curves of b10 samples.

Table 2. MDSC characterization of prepared samples (free grey space in columns denotes that value not been obtained; dash denotes that concrete product is not present in sample).

Sample	T_g [°C]	T_c Sb_2S_3 [°C]		T_c $AgSbS_2$ [°C]		T_c Ag_3SbS_3 [°C]		T_m Sb_2S_3 [°C]		T_m Ag_3SbS_3 [°C]	
		onset	peak	onset	peak	onset	peak	onset	peak	onset	peak
b2-0	221	257.8	265.4	-	-	-	-			-	-
b2-5	175	234.7	239.8	-	-	219.7	227.3	445.8	448.0		
b2-10	180	230.5	236.5	-	-	218.6	223.4	440.3	442.9	373.6	375.7
b10-0	157	179.6	191.2	-	-	-	-			-	-
b10-10	156	185.7	195.6			-	-			-	-
b10-20	153	176.6	180.3			-	-			-	-
b10-30	147	174.8	177.6	154.8	160.2	-	-			-	-
b10-40		182.6	181.4	144.2	149.9	-	-			-	-
b10-50		207.0	211.7	136.3	142.5	-	-			-	-

4. Discussion

Raman spectra (Figs. 1. and 2.) clearly represent differences between prepared thin films (i.e. b2 samples and b10 samples). Raman bands 140 cm^{-1} and 475 cm^{-1} (vibrations of S ring fragments) which are visible in case of b10 samples are not present in case of b2 samples. As well spectra of b2 samples are much more similar to spectra of amorphous films $Sb_{40}S_{60}$ (stoichiometric Sb_2S_3) published in [18]. These results support results of EDX elementary analysis. With increasing silver content is in case of b10 samples visible shift of band 292 cm^{-1} to lower frequencies. Decreasing intensity of bands 140 cm^{-1} and 475 cm^{-1} and increasing intensity of band 170 cm^{-1} is also visible in case of b10 samples with increasing silver content. These results can be explained as disappearing S-S bonds due to bonding of Ag during OIDD.

From optical transmission spectra is visible red shift of short wavelength edge (decreasing of E_g^{opt} (Table 1. and Figs. 3 - 5)) and increasing of modulation amplitude interference curves (increasing of refractive indices (Figs. 3, 4, 6, 7)) with increasing silver content. Decreasing of E_g^{opt} can be explained by fact, that the binding energies [19] of Ag-S (155 $kJ \times mol^{-1}$) and Sb-Sb (175 $kJ \times mol^{-1}$) is smaller than binding energies of Sb-S (260 $kJ*mol^{-1}$) and S-S (280 $kJ \times mol^{-1}$). The same idea can be applied in comparison of b2 ($Sb_{40}S_{60}$) and b10 ($Sb_{33}S_{67}$) samples.

DSC curves (Figs. 8. - 11.) are evaluated on basis of known chemical composition (EDX) of prepared films and XRD identification of products photocrystallized by Ar^+ ion laser exposition [17] together with optically detected photocrystallization kinetic curves (dependences of decreasing transmission on Ar^+ ion laser exposure time) as reported in [17]. Phase diagrams [20,21] were taken to account too.

Samples b2-0 and b10-0 are pure Sb-S system, other samples contains Ag. While crystallization of Ag doped b2 samples produces Ag_3SbS_3 (LT form), crystallization of Ag doped b10 samples produces $AgSbS_2$ (HT form) [17]. Crystalline Sb_2S_3 is present in all samples. From XRD patterns is visible, that in case of b2 samples and b10 samples with low silver concentration crystallization of Sb_2S_3 and Ag-Sb-S product run simultaneously, in case of b10 samples with high Ag content ($c_{Ag} > 8$ at.%) crystallization process consist of two steps. First step is equal to crystallization of $AgSbS_2$ second step to crystallization of Sb_2S_3. This disintegration is identifiable as breaking of single sigmoidal crystallization kinetic curve to two steps [17]. This phenomena can explain the tendency to change the $T_c(Sb_2S_3)$ values.

5. Summary

There were prepared homogeneous amorphous thin films of (Ag)-Sb-S by thermal evaporation of Sb-S combined with optically induced diffusion and dissolution of silver. It is clear, that evaporation rate influences composition of prepared films and consequently structure and maximal silver concentration. With increasing evaporation rate increases sulfur content in prepared films as well as increase concentration limit of photodissolved silver in Sb-S thin films.

With increasing sulfur content in prepared films increase refraction index and decrease E_g^{opt} (red shift). With increasing sulfur content strongly decrease T_g and $T_c(Sb_2S_3)$ values.

With increasing silver content in prepared films decreases intensity of S-S bond and increase intensity of Sb-Sb bond vibrations. Also shift of band equal to Sb-S bond vibrations to lower frequencies is visible. With increasing silver content increase refraction index and decrease E_g^{opt} (red shift).

With increasing silver content decreases T_g value and other characteristic temperatures (T_c and T_m of Sb_2S_3 and Ag-Sb-S products) except changing $T_c(Sb_2S_3)$ values in b10 samples explained by change of simultaneous crystallization in two crystallization steps.

Acknowledgement

Research Centre grant LC523, Grant Agency of Czech Republic grant GA 203/05/524 and University of Pardubice internal grant 3310/20/FG350021 are greatly acknowledged.

References

[1] G. F. Zhou, Mat. Sci. Eng. A **304-306**, 73 (2001).
[2] B. Hyot, L. Poupinet, V. Gehanno, P. J. Desre, J. Magn. Magn. Mater. **249**, 504 (2002).
[3] J. Li, L.Hou, H. Ruan, Q. Xie, F. Gan, Proc. SPIE **4085**, 125 (2001).
[4] H. J. Borg, R. van Woudenberg, J. Magn. Magn. Mater. **193,** 519 (1999).
[5] T. Ohta, J. Optoelectron. Adv. Mat. **3**, 609 (2001).
[6] K. Nagata, K. Nishiuchi, S. Furukawa, N. Yamada, N. Akahira, Jpn. J. Appl. Phys. **38**, 1679 (1999).
[7] M. J. Dekker, N. Pfeffer, M. Kuijper, I. P. D. Ubbens, W. M. J. Coene, E. R. Meinders, H. J. Borg, Proc. SPIE **4090**, 28 (2000).
[8] G. Knight, Data Storage **5**, 23 (1998).
[9] E. Betzig, J. K. Trautman, R. Wolfe, E. M. Gyorgy, P. L. Finn, M. H. Kryder, C. H. Chang, Appl. Phys. Lett. **61**, 142 (1992).
[10] T. Ohta, M. Birukawa, N. Yamada, K. Hirao, J. Magn. Magn. Mater. **242-245, Part 1**, 108 (2002).
[11] S. Ichiura, Y. Tsuchiya, H. Terasaki, O. Ota, Jpn. J. Appl. Phys. **33**, 1357 (1994).
[12] T. Ohta, K. Nishiuchi, K. Narumi, Y. Kitaoka, H. Ishibashi, N. Yamada, T. Kozaki, Jpn. J. Appl. Phys. **39** 770 (2000).
[13] T. Wágner, J. Gutwirth, M. Krbal, Mir. Vlček, Mil. Vlček, M. Frumar: J. Non-Cryst. Solids **326-327**, 238 (2003).
[14] T. Wágner, J. Gutwirth, T. Kohoutek, M. Krbal, P. Bezdička, J. Pokorný, M. Vlček, M. Frumar, Proc. E*PCOS 04, Balzers, 2004, chap. 4. (to be published in J. Non-Cryst. Solids)
[15] R. Swanepoel, J. Phys. E: Sci. Instrum. **16**, 1214 (1983).
[16] J. Tauc, in: J. Tauc (Ed.), Amorphous and Liquid Semiconductors, Plenum, New York (1974).
[17] J. Gutwirth, T. Wágner, P. Bezdička, J. Pokorný, Mil. Vlček, M. Frumar, Proc. ISNOG 14th, Port Cape Canaveral, USA, 2004, p. 82. (to be published in Phys. Chem. Glasses)
[18] I. Watanabe, S. Noguchi, T. Shimizu, J. Non-Cryst. Solids **58**, 35 (1983).
[19] A. Feltz, Amorphous Inorganic Materials and Glasses, VCH Weineheim, Weineheim (1993).
[20] P. Villars, A. Prince, H. Okamoto in Handbook of Ternary Alloy Phase Diagrams Vol. 3, ASM International, (1995).
[21] H. Okamoto P. R. Subramanian, L. Kacprzak in Handbook of Binary Alloy Phase Diagrams Second Edition Vol. 1, ASM International, (1992).